

## Exponentially growing solutions in homogeneous Rayleigh-Bénard convection

E. Calzavarini,<sup>1</sup> C. R. Doering,<sup>2</sup> J. D. Gibbon,<sup>3</sup> D. Lohse,<sup>1</sup> A. Tanabe,<sup>3</sup> and F. Toschi<sup>4</sup>

<sup>1</sup>*Department of Applied Physics, University of Twente, 7500 AE Enschede, The Netherlands*

<sup>2</sup>*Department of Mathematics and Michigan Center for Theoretical Physics, University of Michigan, Ann Arbor, Michigan 48109-1043, USA*

<sup>3</sup>*Department of Mathematics, Imperial College London, London SW7 2AZ, United Kingdom*

<sup>4</sup>*IAC-CNR, Istituto per le Applicazioni del Calcolo, Viale del Policlinico 137, I-00161 Roma, Italy and INFN, Via Paradiso 12, I-43100 Ferrara, Italy*

(Received 23 September 2005; published 17 March 2006)

It is shown that homogeneous Rayleigh-Bénard flow, i.e., Rayleigh-Bénard turbulence with periodic boundary conditions in all directions and a volume forcing of the temperature field by a mean gradient, has a family of exact, exponentially growing, separable solutions of the full nonlinear system of equations. These solutions are clearly manifest in numerical simulations above a computable critical value of the Rayleigh number. In our numerical simulations they are subject to secondary numerical noise and resolution dependent instabilities that limit their growth to produce statistically steady turbulent transport.

DOI: [10.1103/PhysRevE.73.035301](https://doi.org/10.1103/PhysRevE.73.035301)

PACS number(s): 47.27.T–

Much effort has been expended in recent decades in addressing the problem of heat transfer in Rayleigh-Bénard thermal convection cells [1]. An asymptotic high Rayleigh number heat transport scaling behavior  $Nu \sim Ra^{1/2}$  (perhaps with logarithmic modifications), with  $Nu = Q(\kappa\Delta T/H)^{-1}$  dimensionless heat flux and  $Ra = \alpha g H^3 \Delta T (\nu\kappa)^{-1}$ , has been conjectured as the ultimate regime [2–5,7]. While current experimental data for high Rayleigh numbers are controversial [8–12], numerical simulations have not been very effective in studying this regime because of difficulties in dealing with the huge number of degrees of freedom engendered when Rayleigh numbers reach the order of at least  $10^{12}$ . Recently, some of us [5,6] have studied a triperiodic convective cell, or homogeneous Rayleigh-Bénard (HRB) system, in order to bridge such difficulties, and to investigate the properties of the convective cell once the effect of boundary layers has been eliminated. Model systems of this sort with hyperviscosity were first investigated computationally by Borue and Orszag [13], and later by Celani *et al.* (in two spatial dimensions) [14] with hyperviscosity and extra large scale dissipation as well.

In this Rapid Communication we point out some peculiar properties of the HRB model that are particularly striking in the low Rayleigh number regime, the opposite regime from that studied in Refs. [5,6]. First we display a family of exact, exponentially growing, separable solutions of the full nonlinear HRB system. We show that these solutions are clearly manifest in direct numerical simulations in the Rayleigh number regime above a computable critical value. Then by way of a careful numerical precision study we show that these may be robust and attracting solutions of the full system of partial differential equations.

Here we would like to anticipate that recently a cleverly conducted series of experiments was designed such as to reduce the influence of top and bottom plates on the physical core of thermal convection [15]. In these experiments the temperature gradient in the bulk of the cell is not imposed but rather, as in fixed-flux convection [16], measured as a

dependent parameter. Interestingly, the  $Nu \sim Ra^{1/2}$  and  $Re \sim Ra^{1/2}$ ,  $Re = u_{rms}(L\nu)^{-1}$ , scalings observed are consistent with HRB simulations in Refs. [5,6].

The system to be studied is described in terms of the following partial differential equations

$$\mathbf{u}_t + \mathbf{u} \cdot \nabla \mathbf{u} + \nabla p = \nu \Delta \mathbf{u} + k \alpha g \theta, \quad (1)$$

$$\theta_t + \mathbf{u} \cdot \nabla \theta = \kappa \Delta \theta + \frac{\Delta T}{H} u_z, \quad (2)$$

where  $\mathbf{u} = (u_x, u_y, u_z)$  is an incompressible velocity field,  $\nabla \cdot \mathbf{u} = 0$ ,  $\nu$ ,  $\kappa$ , and  $\alpha g$  are, respectively, the kinematic viscosity, thermal diffusivity, and the thermal expansion coefficient times the acceleration due to gravity. These equations are used to describe the evolution of the velocity field in a triply periodic cubic volume  $[0, H]^3$  in the presence of a temperature field  $T(\mathbf{x}, t) = \bar{T}(\mathbf{x}) + \theta(\mathbf{x}, t)$ . The temperature is expressed as a fluctuation  $\theta$  with respect to a mean profile  $\bar{T}(\mathbf{x})$  that is imposed to be equal to the mean conductive temperature profile in such a Rayleigh-Bénard cell; i.e., linear and of the form  $\bar{T}(\mathbf{x}) = -z\Delta T/H + \frac{1}{2}\Delta T$ .

When nondimensionalizing lengths with  $H$ , velocities with  $\kappa/H$ , and temperatures with  $\Delta T$ , Eqs. (1) and (2) can be rewritten as

$$\mathbf{U}_t + \mathbf{U} \cdot \nabla \mathbf{U} + \nabla P = \text{Pr}(\Delta \mathbf{U} + \mathbf{k} \text{Ra} \Theta), \quad (3)$$

$$\Theta_t + \mathbf{U} \cdot \nabla \Theta = \Delta \Theta + w, \quad (4)$$

where  $\Theta$ ,  $P$ , and  $\mathbf{U} = (u, v, w)$  are the dimensionless temperature, pressure, and velocity fields, respectively, and  $\text{Pr} \equiv \nu/\kappa$  and  $\text{Ra} \equiv \alpha g H^3 \Delta T (\nu\kappa)^{-1}$  are the Prandtl and Rayleigh numbers. In this system periodic boundary conditions are imposed on *all* the dependent variables on the cube  $[0, 1]^3$ . We consider the equations of motion (3) and (4) with spatially mean-zero initial data for all  $\mathbf{U}$  and  $\Theta$  so that solutions subsequently remain spatially mean-zero at all times.

With these boundary conditions there is a family of non-linear “separable” solutions of (3) and (4) where  $\mathbf{U}$ ,  $\Theta$ , and  $P$  are functions only of  $x$ ,  $y$ , and  $t$  but not of the vertical coordinate  $z$ . To see this, let  $\mathbf{v} = \mathbf{i}u(x,y,t) + \mathbf{j}v(x,y,t)$  and  $P = q(x,y,t)$ . Then the divergence-free velocity  $\mathbf{v} = (u, v)$ , and  $q$ ,  $w$ , and  $\Theta$  satisfy

$$\mathbf{v}_t + \mathbf{v} \cdot \nabla \mathbf{v} + \nabla q = \text{Pr} \Delta \mathbf{v}, \quad (5)$$

$$w_t + \mathbf{v} \cdot \nabla w = \text{Pr}(\Delta w + \text{Ra} \Theta), \quad (6)$$

$$\Theta_t + \mathbf{v} \cdot \nabla \Theta = \Delta \Theta + w. \quad (7)$$

Equation (5) is the unforced two-dimensional Navier-Stokes equation whose solutions decay to zero exponentially in time [17]. As  $\mathbf{v}$  decays away, Eqs. (6) and (7) admit *exact* solutions of the form

$$\begin{bmatrix} w(x,y,t) \\ \Theta(x,y,t) \end{bmatrix} = \begin{bmatrix} w_0 \\ \Theta_0 \end{bmatrix} e^{\lambda t} \sin(k_x x + k_y y + \phi), \quad (8)$$

with the growth rate

$$\lambda = -\frac{1}{2}(\text{Pr} + 1)k^2 + \frac{1}{2}\sqrt{(\text{Pr} + 1)^2 k^4 + 4\text{Pr}(\text{Ra} - k^4)} \quad (9)$$

and where  $\phi$  is an arbitrary phase. Therefore, for  $\text{Ra}$  above a critical value  $\text{Ra}_c = k^4 = (2\pi)^4$  the exponential solutions are unbounded; i.e.,  $\lambda > 0$ . Since  $\mathbf{k} = 2\pi(n_x, n_y)$ , where  $n_{\{x,y\}}$  are ( $\pm$ )-integer wave numbers, we can relabel the exponent  $\lambda$  as  $\lambda(n_x, n_y)$ . Degenerate values of  $\lambda(n_x, n_y)$  are possible, corresponding to different combinations of  $n_x, n_y$ . The number of positive  $\lambda$  grows asymptotically  $\sim \text{Ra}^{1/2}$ . These solutions actually transport unlimited heat because  $\text{Nu} \sim \langle w\Theta \rangle \sim \exp(2\lambda t)$ . Such runaway solutions and their possible instabilities may be actually the dominant features of the simulations in Refs. [13,14], and in Refs. [5,6] where a  $\text{Nu} \sim \text{Ra}^{1/2}$  dependence was observed. Therefore, the relevance of computations on periodic domains as models for the bulk of systems with essential boundaries may be arguable. Indeed, Borue, and Orszag [13] seemed to hint at this issue when they remarked “It turns out that in homogeneous convection [the heat transport, temperature and velocities] are strongly fluctuating and intermittent in time. This fact makes reliable measurements of [these variables] difficult.”

One of the purposes of this paper is to show that solutions in (8) appear to be attracting and may dominate the dynamics in numerical integrations of Eqs. (1) and (2) on fully periodic domains at low  $\text{Ra}$  numbers. Resolution and precision difficulties, however, prevent us from drawing firm conclusions about the physics behind secondary instabilities that limit the growth of the runaway solutions to produce statistically steady turbulent transport in simulations at higher  $\text{Ra}$ . This remains an open question subject to further, deeper, investigations.

Indeed while unlimited heat transport could be expected because of the solutions (8), even at moderately low Rayleigh numbers simulations of the homogeneous convective system display a statistically stationary behavior where the growing modes, when they appear, break up due to rapid destabilization (we limit our investigation to the  $\text{Pr}=1$  case).

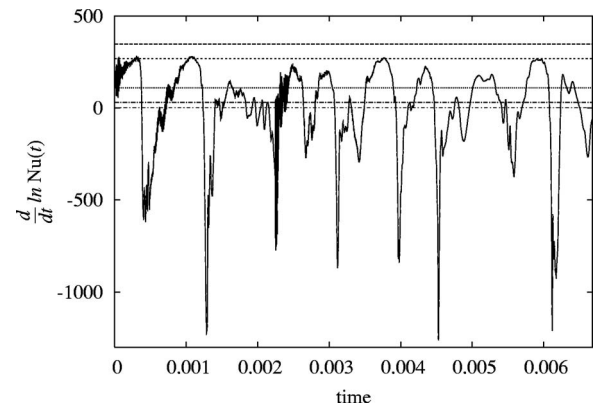


FIG. 1. Derivative with respect to time of the logarithm of  $\text{Nu}(t)$ , in a homogeneous convective system at  $\text{Ra} = 4.5 \times 10^4 \approx 30\text{Ra}_c$ . The direct numerical simulation (DNS) is implemented through a Lattice Boltzmann equation (LBE) algorithm on a cubic grid with resolution  $240^3$ , as in Refs. [5,6]. Horizontal lines, from top to bottom, correspond respectively to values  $2\lambda(0,1)$ ,  $2\lambda(1,1)$ ,  $2\lambda(0,2)$ ,  $2\lambda(0,2)$ , and the zero level. The time, here and in the following figures, is dimensionless as for the set of Eqs. (3) and (4), i.e., it has been normalized by the thermal diffusion time across the box,  $H^2/\kappa$ .

Figure 1 shows the time derivative of the logarithm of the Nusselt number [i.e., the volume average  $\text{Nu}(t) = \langle w\Theta \rangle_V$ ] for  $\text{Ra} \approx 4.5 \times 10^4$ . The growth rate of  $\text{Nu}(t)$  appears to bounce between some of the admissible exponential modes, although in these simulations the fastest growing modes,  $\lambda(0, \pm 1)$  and  $\lambda(\pm 1, 0)$ , are never reached. The numerical results in Fig. 1 were obtained by means of a LBE algorithm at a relatively high resolution,  $240^3$  (see Ref. [6] for details). The value of  $\text{Ra}$  adopted here is a little below, but of the same order as, the lower values of  $\text{Ra}$  for data analyzed in Ref. [6].

To better understand the relevant features of the dynamics of the exponentially growing solutions we have performed a series of DNS at values of  $\text{Ra}$  only slightly above the critical value ( $\text{Ra} \geq \text{Ra}_c$ ) where just *one* distinct positive value of  $\lambda$  exists. These integrations were performed by means of a fully dealiased pseudospectral algorithm that allows for more flexibility. It allows the adjustment of the time step size that is implicitly fixed by the spatial grid in the LBE, and gives clearer control of the scales involved in the dynamics. Furthermore, because we are interested here in the low- $\text{Ra}$  regime, it is reasonable to perform numerical simulations with lower resolutions (i.e.,  $32^3$  or  $64^3$ ). Nevertheless, we caution that in case of unlimited exponential growth *any* spatial resolution may be insufficient at some point in time.

Figure 2 displays the temporal behavior of the global (spatial) rms values of the three velocity components. For clarity the temperature  $\Theta$  has been omitted from the figure because it is strongly correlated with  $w$ , almost coincident with it. As expected from the unstable analytic solution,  $w$  grows at an exponential rate  $\propto \exp(\lambda t)$  while the horizontal components ( $u, v$ ) rapidly decrease.

The plateaux in Fig. 1 and the linear growth (on the linear-log scale) in Fig. 2 indicate the presence of exponentially growing solutions, but it is difficult to determine the nature of the sudden departures from this state. Secondary

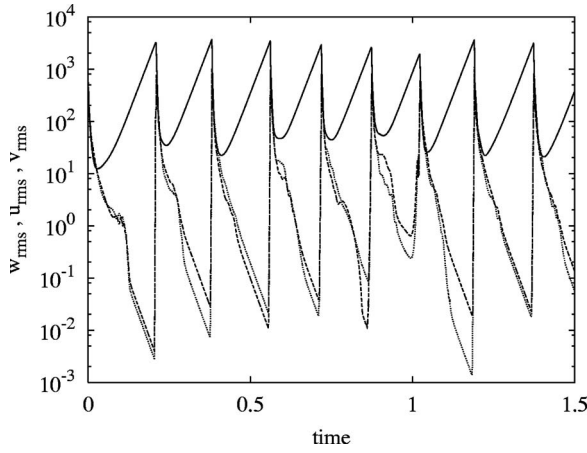


FIG. 2. Linear-log plot of the spatial rms value of the three velocity component and the thermal fluctuation in the DNS at resolution  $32^3$ ,  $w_{rms}$  (solid),  $u_{rms}$  (dashed), and  $v_{rms}$  (dotted).

instabilities are necessary to limit the growth of the runaway solutions and produce  $z$ -dependent states that represent steady turbulent transport. However, Fig. 3 is a comparison between floating point and double precision calculations for the mean squared velocity components indicating the sensitivity of the exponential solutions to random perturbations generated by round-off noise and discretization errors.

The simulations indicated that the breakdown of the exponentially growing solutions for  $w$  and  $\Theta$  and the exponentially decaying solutions for  $u$  and  $v$  is first signaled in these horizontal components. It is not clear at this point what are the relevant scales involved in this process for  $Ra \geq Ra_c$ , although we observe that the growth of the horizontal components destabilizes the exponentially growing modes, leading to a fast redistribution of energy at all scales. At the peak, when  $w$  and  $\Theta$  reach their maxima, almost flat energy spectra are produced irrespective of the resolution adopted. Subsequently the high wave vector dissipation takes over and the process is repeated, repeating the previous exponential growth. In summary, our simulations suggest that the expo-

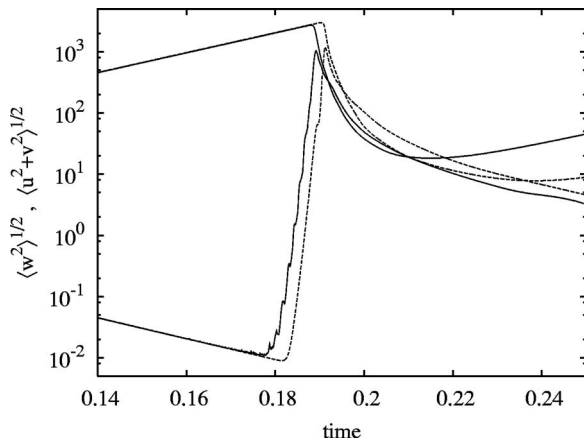


FIG. 3. A comparison between floating point (solid) and double precision (dashed) calculations for the root mean squared velocity component  $w$ , and  $\langle u^2 + v^2 \rangle^{1/2}$  vs time, with spatial resolution  $32^3$  and second order Adams-Bashforth as time marching algorithm.

ponential solutions may in fact be attracting for a broad class of initial conditions, although subject to some finite amplitude instabilities.

There are other problems where extreme limits of models introduce runaway solutions such as those appearing here. A distinct example is zero-Prandtl number Rayleigh-Bénard convection [18,19] where the singular limit of the Boussinesq equations admits exponentially growing solutions even in the presence of rigid (albeit free-slip) boundaries. It was long ago observed in double diffusive convection in the absence of rigid boundaries that linearly unstable modes representing “salt fingers” are exact solutions of the nonlinear equations [20,21].

Another model implemented with fully periodic conditions to avoid boundary layers, in which a similar nonlinear separation of variables appears, is shear-driven turbulence. In that model the fluctuations about an imposed mean shear flow  $\mathbf{i}Sy$  obey

$$u_t + u \cdot \nabla u + Sy \partial_x u + \mathbf{i}Sv + \nabla p = \nu \Delta u. \quad (10)$$

Fully periodic conditions cannot be implemented directly here, though, due to the presence of the incompatible operator  $Sy \partial_x$  (explicitly nonperiodic in  $y$ ). It was noted [22] that periodic conditions *can* be imposed on independent variables  $x' = x - Syt$ ,  $y' = y$ ,  $z' = z$ , and  $t' = t$ , and this transformation has been used to perform numerical simulations of “homogeneous shear flow” [23].

These periodic conditions also allow for an exact nonlinear separation of the cross-stream and stream-wise components. Indeed, the change of variables implies

$$\nabla \rightarrow \nabla' - \mathbf{j}St \partial_{x'} \text{ and } u_t + Sy \partial_x u = u_{t'}. \quad (11)$$

Thus, acting on functions *only* of  $y'$ ,  $z'$ , and  $t'$ , the operators  $\nabla = \nabla' = \mathbf{j} \partial_{y'} + \mathbf{k} \partial_{z'}$ , and  $\Delta = \Delta' = \partial_{y'}^2 + \partial_{z'}^2$ . Hence, the system (10) separates for solutions depending only on  $y'$ ,  $z'$  and  $t'$ : the two-dimensional divergence-free velocity fields  $\mathbf{v} = \mathbf{j}v(y', z', t') + \mathbf{k}w(y', z', t')$  and pressure  $p(y', z', t')$  satisfy the unforced Navier-Stokes equation

$$v_t + v \cdot \nabla' v + \nabla' p = \nu \Delta' v, \quad (12)$$

and the stream-wise component  $u(y', z', t')$  evolves according to the linear inhomogeneous equation

$$u_t + v \cdot \nabla' u + Sv = \nu \Delta' u. \quad (13)$$

These equations do not (apparently) support unbounded exponentially growing fields but they do display non-normal transient growth among their fully nonlinear exact solutions. Indeed, the decaying solutions of (12)

$$v = \Omega e^{-\nu(k_2^2 + k_3^2)t'} \sin(k_2 y' + k_3 z' + \phi) [\mathbf{j}k_3 - \mathbf{k}k_2] \quad (14)$$

produce a stream-wise flow of the form

$$u = (U - \Omega S k_2 t') e^{-\nu(k_2^2 + k_3^2)t'} \sin(k_2 y' + k_3 z' + \phi), \quad (15)$$

where  $U$  and  $\Omega$  are set by initial conditions. The peak amplitude  $u_{peak} = -e^{-1} \Omega S k_3 / \nu(k_2^2 + k_3^2)$  (when  $U=0$ ) may be extremely large at high Reynolds number when  $S k_3 / \nu(k_2^2 + k_3^2) \gg 1$ . This is consistent with the behavior reported by Pumir and Shraiman based on their direct numeri-

cal simulations [23]: “The transient regime is characterized by a violent growth of the kinetic energy... While this growth eventually stops...the turbulent regime that follows exhibits large fluctuations of spatially averaged quantities... Because of the unusually large level of fluctuations, very long runs are necessary to get steady averages, which explains why we chose to work at moderate resolution.”

We conclude that the imposition of periodic boundary conditions may admit an exact nonlinear separability that allows for larger fluctuations than are possible in the presence of rigid boundaries. In full three-dimensional simulations of some of these systems, secondary instabilities are the only limiting processes that can lead to finite statistically steady turbulent transport. Among the delicate—and currently unresolved—issues is the question of how sensitive the statistics of high Ra (or Re) simulations may be to numerical discretization and noise. Nevertheless the HRB

model, although physically unrealizable because of the boundary conditions, has stimulated interesting experiments [15] where the effect of the thermal boundaries has been reduced to reveal the  $Nu \sim Ra^{1/2}$  scaling observed in the high Rayleigh number simulations [5,6].

We thank B. Castaing for useful discussions and for sharing their results prior to publication. E.C. thanks A. Sevilla for many useful discussions. This work is part of the research program of FOM, which is supported by NWO and by the European Union (EU) under Contract No. HPRN-CT-2000-00162. C.R.D. was supported in part by NSF-PHY0244859 and by the Alexander von Humboldt Foundation. A.T. has been supported by ORS. C.R.D., J.D.G., and A.T. acknowledge the hospitality of the 2005 Program in Geophysical Fluid Dynamics at Woods Hole Oceanographic Institution where part of this work was completed.

- 
- [1] L. P. Kadanoff, *Phys. Today* **54**, 34 (2001).  
 [2] R. H. Kraichnan, *Phys. Fluids* **5**, 1374 (1962).  
 [3] E. A. Spiegel, *Annu. Rev. Astron. Astrophys.* **9**, 323 (1971).  
 [4] S. Grossmann and D. Lohse, *J. Fluid Mech.* **407**, 27 (2000); *Phys. Rev. Lett.* **86**, 3316 (2001); *Phys. Fluids* **16**, 4462 (2004).  
 [5] D. Lohse and F. Toschi, *Phys. Rev. Lett.* **90**, 034502 (2003).  
 [6] E. Calzavarini, D. Lohse, F. Toschi, and R. Tripiccione, *Phys. Fluids* **17**, 055107 (2005).  
 [7] L. N. Howard, *J. Fluid Mech.* **17**, 405 (1963); C. R. Doering and P. Constantin, *Phys. Rev. E* **53**, 5957 (1996).  
 [8] X. Chavanne, F. Chillà, B. Castaing, B. Hebral, B. Chabaud, and J. Chaussy, *Phys. Rev. Lett.* **79**, 3648 (1997).  
 [9] J. Glazier, T. Segawa, A. Naert, and M. Sano, *Nature (London)* **398**, 307 (1999).  
 [10] J. Sommeria, *Nature (London)* **398**, 294 (1999).  
 [11] P.-E. Roche, B. Castaing, B. Chabaud, and B. Hebral, *Phys. Rev. E* **63**, 045303(R) (2001).  
 [12] F. Chillà, M. Rastello, and S. Chaumat, *Phys. Fluids* **16**, 2452 (2004).  
 [13] V. Borue and S. A. Orszag, *J. Sci. Comput.* **12**, 305 (1997).  
 [14] A. Celani, T. Matsumoto, A. Mazzino, and M. Vergassola, *Phys. Rev. Lett.* **88**, 054503 (2002).  
 [15] M. Gibert, H. Pabiou, F. Chillà, and B. Castaing, *Phys. Rev. Lett.* (to be published).  
 [16] J. Otero, R. W. Wittenberg, R. A. Worthing, and C. R. Doering, *J. Fluid Mech.* **473**, 191 (2002).  
 [17] C. R. Doering and J. D. Gibbon, *Applied Analysis of the Navier-Stokes Equations* (Cambridge University Press, Cambridge, 1995).  
 [18] E. A. Spiegel, *J. Geophys. Res.* **67**, 3063 (1962).  
 [19] O. Thual, *J. Fluid Mech.* **240**, 229 (1992).  
 [20] M. E. Stern, *Tellus* **12**, 172 (1960).  
 [21] J. S. Turner, *Annu. Rev. Fluid Mech.* **6**, 37 (1974).  
 [22] R. S. Rogallo, NASA Tech. Memo. 81315 (1981).  
 [23] A. Pumir and B. I. Shraiman, *Phys. Rev. Lett.* **75**, 3114 (1995).